Biophysical Chemistry 162 (2012) 14–21

Contents lists available at SciVerse ScienceDirect

Biophysical Chemistry

journal homepage: http://www.elsevier.com/locate/biophyschem

Indium Tin Oxide devices for amperometric detection of vesicular release by single cells

Anne Meunier [a], Rémy Fulcrand [a], François Darchen [b], Manon Guille Collignon [a], Frédéric Lemaître [a], Christian Amatore [a,*]

[a] Ecole Normale Supérieure, Département de Chimie, UMR CNRS-ENS-UPMC 8640 « PASTEUR », 24 rue Lhomond, 75231 Paris cedex 05. France
[b] CNRS/Université Paris Descartes UMR8192, 45 rue des Saints-Pères, 75270, Paris cedex 06, France

HIGHLIGHTS

- Microfabrication of three microsystems for amperometric detection of exocytosis.
- Effect of collagen treatments on the electrochemical capability.
- Moderate collagen treatment does not induce any alteration of voltammetric responses or degradation of the signal-to-noise ratio.

GRAPHICAL ABSTRACT

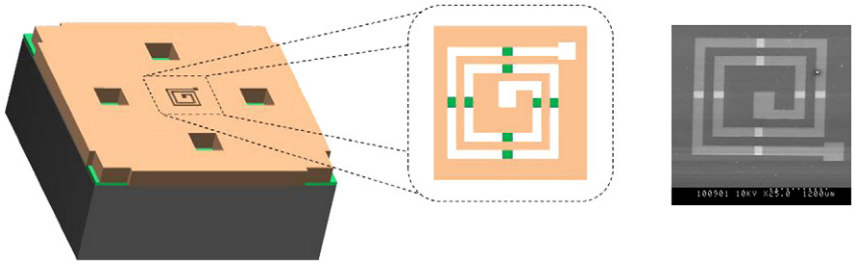

ARTICLE INFO

Article history:
Received 26 October 2011
Received in revised form 9 December 2011
Accepted 18 December 2011
Available online 24 December 2011

Keywords:
Exocytosis
Amperometry
Indium Tin Oxide microelectrode
Microsystem
Collagen surface treatment

ABSTRACT

The microfabrication and successful testing of a series of three ITO (Indium Tin Oxide) microsystems for amperometric detection of cells exocytosis are reported. These microdevices have been optimized in order to simultaneously (i) enhance signal-to-noise ratios, as required electrochemical monitoring, by defining appropriate electrodes geometry and size, and (ii) provide surface conditions which allow cells to be cultured over during one or two days, through apposite deposition of a collagen film. The intrinsic electrochemical quality of the microdevices as well as the effect of different collagen treatments were assessed by investigating the voltammetric responses of two classical redox systems, $Ru(NH_3)_6^{3+/2+}$ and $Fe(CN)_6^{3-/4-}$. This established that a moderate collagen treatment does not incur any significant alteration of voltammetric responses or degradation of the excellent signal-to-noise ratio.
Among these three microdevices, the most versatile one involved a configuration in which the ITO microelectrodes were delimited by a microchannel coiled into a spiral. Though providing extremely good electrochemical responses this specific design allowed proper seeding and culture of cells permitting either single cell or cell cluster stimulation and analysis.

1. Introduction

Vesicular exocytosis is a key biological mechanism allowing cell communication by release of bioactive molecules into extracellular medium. As such, the exact delineation of the main factors which command this crucial phenomenon has been the target of numerous investigations. It is now generally assumed that secretory vesicles filled with specific chemical messengers (neurotransmitters, hormones, peptides) are transported via the cytoskeleton network up to cell membranes where they eventually dock and fuse to release their content into the external medium after adequate stimulation [1]. Yet the exact details of each of these steps, especially those which control the fusion mechanism are still not fully understood. This has prompted the development of several specific physico-chemical

* Corresponding author. Tel.: +33 1 4432 3388; fax: +33 1 4432 3863.
E-mail address: Christian.Amatore@ens.fr (C. Amatore).

0301-4622/$ – see front matter © 2011 Elsevier B.V. All rights reserved.
doi:10.1016/j.bpc.2011.12.002

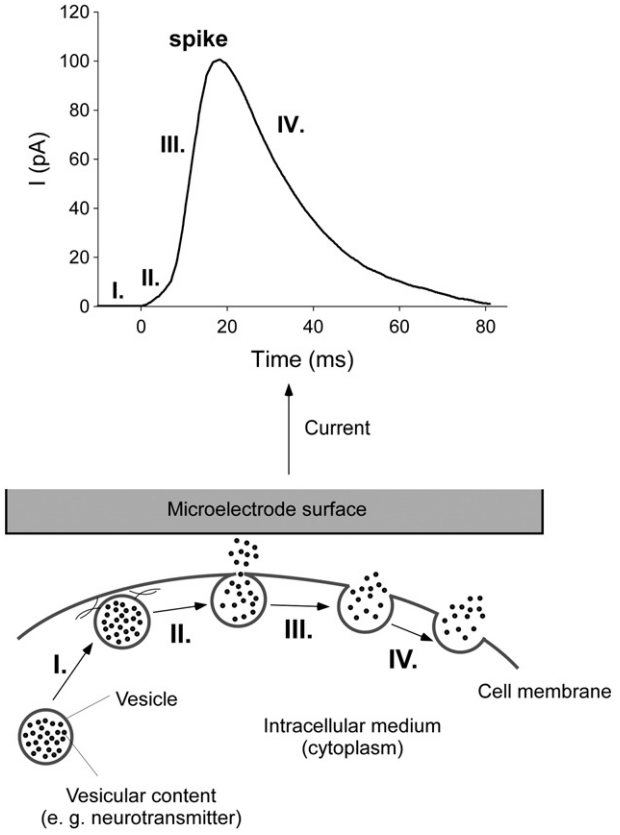

Fig. 1. Top: Representative amperometric spike depicted with the different steps of exocytosis phenomenon. Bottom: Scheme of the successive stages of exocytosis in a cell from vesicle displacement up to fusion of cell and vesicle membranes (docking of the vesicle (I.); formation of the fusion pore (II.); expansion of the pore (III.); massive release (IV.)).

methods which have unravelled essential elements [2–4]. However, none of these methods can provide a complete understanding on their own. This clearly claims for the design of systems allowing the simultaneous recording of vesicular exocytosis by at least two methods, e.g., electrophysiological (patch-clamp), optical and electrochemical [5–8].

Over the last decades, among all the methods developed for real-time investigations at the single living cell level, amperometry at carbon fiber microelectrodes (usually named CFA for Carbon Fiber Amperometry) established itself as one main method for allowing the quantitative monitoring of exocytotic release with an excellent temporal resolution, particularly for analyzing individual secretory events [5,9,10]. In the most common configuration, a carbon fiber microelectrode is positioned in nanometric contact to the surface of the investigated cell and polarized at an appropriate potential for oxidizing the electroactive molecules contained in the vesicular efflux. The released molecules fastly diffuse across the cell-electrode cleft to reach the electrode surface where they are detected through their electrochemical oxidation. Amperometric signals thus display a succession of current spikes. Each of these spikes features one vesicular event and its morphology and intensity are related to the sequential dynamics of release (kinetics and quantum of charge) from an individual vesicle (Fig. 1) [5].

Despite its great simplicity and success, amperometry has several intrinsic limitations. First of all, amperometry is naturally blind to non-electroactive substances. Even when this point can be solved using modified electrodes [11,12], amperometric detection requires that molecules reach the electrode electroactive surface, so amperometry is also blind to any phenomenon that precedes the secretory event itself (displacements of the vesicles, docking location, etc.). This is why numerous works have been recently devoted to integrating amperometry with others complementary real-time techniques like patch-clamp (which records events even if the released molecules are not electroactive) or/and optical fluorescence microscopy (which allows visualizing vesicles into the intracellular medium). Another drawback of amperometry is ironically due to one of its main advantages, viz., its excellent performance for single cell analyses. Actually, reporting statistically significant information implies overcoming the cellular variability and hence requires a huge and time-consuming number of experiments. During the last years, microsystems designed to achieve parallel recordings from multiple cells have blossomed, as recently reported in excellent reviews [13–16]. Notably, they have been designed based on microelectrodes arrays [17–20] or microelectrodes integrated in microchannels [21–24] or microwells [25–29]. Among them, a few microwell-based devices allowed amperometric signals from different releasing zones to be identified [20,30,31]. In the context of the present work it is worth mentioning that some of these microdevices were also designed to allow coupling between amperometry and electrophysiological or optical measurements of exocytosis [21,22,28,32,33].

Carbon fiber amperometry collects vesicular release information from the apical pole of cells investigated. Conversely, the above mentioned microdevices are generally designed to allow measurements of secretion from “basal pole” of cells, i.e., from the cellular region adherent to the underlying substratum. In that sense, a great attention needs to be devoted to ensure the quality of cellular adhesion because this ultimately determines the significance of the monitored secretory activity. Moreover, the total surface of the device could be not homogenous (the electrode surface could be only a portion of the whole surface, see below). To maintain a close contact between the cell membrane and the electrode, the surface of the electrode must allow efficient cell adhesion. To achieve this requirement, adequate surface treatments are essential as well as to ensure the biological relevance of the studies [34]. However, such treatments may deteriorate the electrochemical properties of the devices compared to CFA. Though, studies investigating this subject are rather scarce.

In order to solve these questions, we have developed hereafter three new microsystems which derive from previous prototypes [32] based on ITO (Indium Tin Oxide) materials. Indeed, among the different materials of electrodes used for electrochemical detections, ITO became very popular due to its ability for optical (transparency) [22,35] and electrochemical (conductivity) recordings [36–38]. In order to preserve future optical applications, ITO has been considered here. Before that, we focus hereafter on electrochemical properties of ITO microelectrodes.

2. Microfabrication and electrochemical properties of microdevices-on-chip (MDOC)

2.1. Microfabrication and comparison of three MDOCs

Transparent ITO coverslips of 100–150 nm thickness have been selected here for the devices fabrication. Yet, the designs presented below are not limited to ITO since other electrode materials may also be used for amperometric monitoring of exocytotic release at the basal pole of the cells [34].

Precise amperometric measurements do not only need electrode materials with excellent electrical conductivity and adequate electrochemical properties but also electrode surface areas small enough to minimize non-faradic information such as electrical noise and capacitive currents. Though, electrodes need to remain large enough for allowing a quantitative collection of released molecules from hot points distributed on the surface of a single cell or from a collection of cells depending on the scope of the measurements.

A compromise between these conflicting requirements can be provided by using ITO microelectrode wells (about 100 μm in diameter), as previously reported in the literature [25,26,33]. Despite their efficiency, these prototypes were not adequate for routine

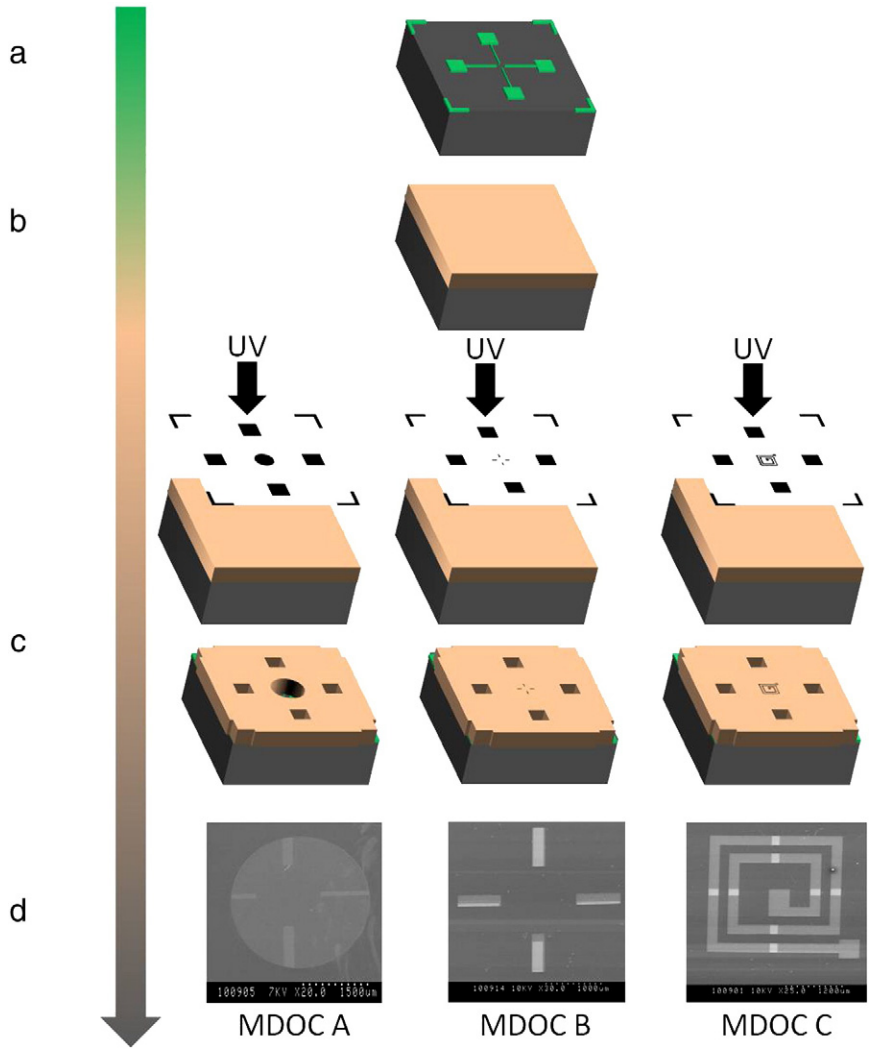

Fig. 2. Representation of the different steps in the photolithographic process to build the MDOC A-C with the resist SU8 to restrict the active surface of ITO band electrodes. a) ITO array band electrodes; b) SU-8 3010 deposition; c) UV exposure and development through masks; d) Optical photographs of the final devices (See Table S1 in Supporting Information for characteristic dimensions).

measurements of single cell secretion because the probability of seeding one or few isolated cells on the exposed electroactive ITO area resulted too weak (approximately once per ten trials). To remediate this situation a series of three microdevices-on-chip (MDOC) have been constructed (MDOC A-C, Fig. 2). All were microfabricated from the same array of four independently addressable ITO bands (200 μm width, 150 nm thick) which were patterned from ITO glass slides by soft photolithography and acid treatment (see Materials and methods) [32]. The whole surface of the glass slide, including the four band-array was first completely insulated with a SU-8 photo-resist and a second photolithographic stage then allowed exposing different lengths, shapes and configurations of the underlying ITO bands and of the surrounding glass substrate upon using three different masks (see Fig. 2 and Material and methods). In MDOC A, the mask allowed removing a disk area (2.6 mm diameter) of the SU-8 resist located in the center of the microsystem so as to expose both the terminal shafts of the four ITO over a length of ca. 700 μm and the glass substrate. In MDOC B, the mask was composed of four rectangles aligned with the band shafts so that the SU-8 resist was only removed over the terminal ends of each ITO band (still over a length of 700 μm) but let the surrounding glass substrate covered. In this configuration, the exposed ITO bands resulted identical to those in MDOC A except that in MDOC B each one lied at the bottom of a rectangular well (Fig. 2) rather than protruding over a comparatively large glass disk. In MDOC C the mask was designed to carve a spiral-like microchannel of 200 μm width in the SU-8 resist layer. This microchannel crossed perpendicularly the ITO bands at periodic instances (Fig. 2) thus exposing a series of squared ITO sections (200 μm × 200 μm) lying on the glass floor of the spiraling microchannel.

MDOC A configuration demonstrated excellent electrochemical properties but the exposed surface area of glass relative to that of ITO bands was too large with the result that seeded cells mostly adhered to the glass floor (vs. only 1–3 cells on each ITO band). MDOC B and MDOC C exhibited also excellent electrochemical behavior as expected since the exposed ITO surface areas were identical to that in MDOC A for MDOC B and smaller for MDOC C. Yet, in MDOC B cells had a spontaneous tendency to cluster onto the ITO electrodes due to their tendency to avoid SU-8 surfaces. This prevented single cell stimulation and analysis and was also not optimal for monitoring events from populations because the cell clusters were not reproducible from run to run. Conversely, when seeding cells in MDOC C the spiraling microchannel pattern spontaneous drove them through the alternating glass and ITO surfaces sequence preventing their aggregation onto the ITO bands. In addition, since the ratio of the overall surface area of exposed ITO electrodes relative to that of the glass sections of the microchannel floor was much increased vs. MDOC A, the probability of spontaneous cell adhesion on ITO increased and ensured that after each seeding several single cells rested on each

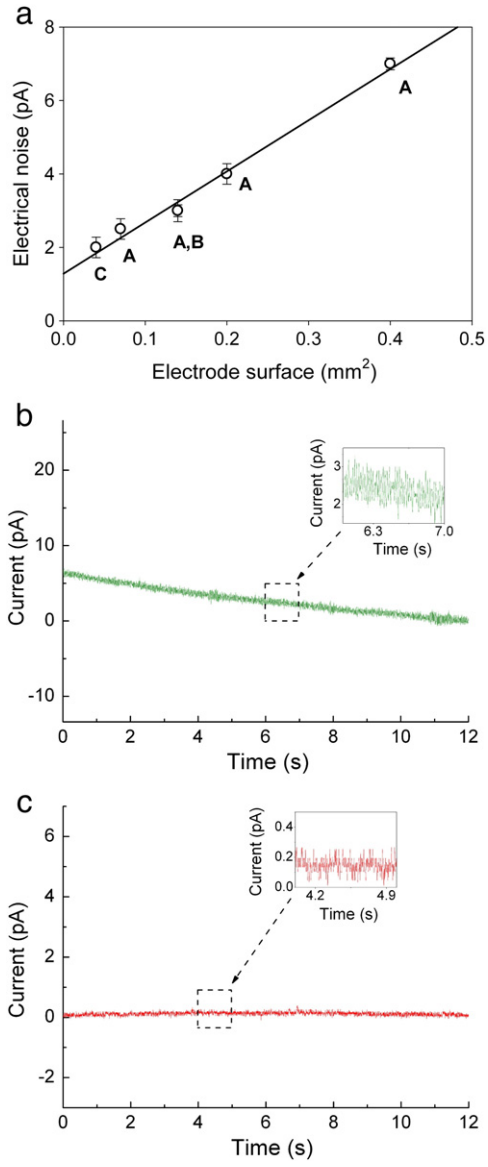

Fig. 3. Measurements of the electrical noise obtained in physiological buffer (Locke's solution, see Materials and methods) at a constant potential value (E = +650 mV vs. Ag/AgCl): a) for different microsystems as a function of electrodes dimensions ($y = 13.93x + 1.284$, $R^2 = 0.986$). Please note that the range of surfaces investigated here has been obtained using the three devices (A, B and C). The type of devices used is depicted in the graph. The error bars represents s.e.m (standard error of the mean) values (n = 3); b) for naked ITO electrode surface on MDOC C; c) for ITO electrode surface covered by cells (in average ca. 20) on MDOC C.

squared ITO electrodes. Hence, MDOC C was retained as optimal, and the further treatments implemented to guarantee proper cellular adhesion viability will be described hereafter only for this microdevice.

2.2. Electrochemical noise levels in MDOCs

Measurements of electrical noise were performed on the three different MDOCs in a Locke's solution appropriate for living cell analysis. Fig. 3A shows that the noise varied linearly with the surface area irrespective of the exact configuration. As expected, MDOC C (ITO surface area of 0.04 mm²) provided the best electrical properties with a rms noise detected by amperometry being typically 1 or 2 pA (Fig. 3B) confirming that the origin of the main electrochemical noise is capacitive. After adhesion of living cells, the free ITO surface decreased so that the rms noise reached a mean value between 0.2 and 1 pA depending on the cell density (Fig. 3C), being then perfectly adequate for precise and accurate amperometric monitoring of exocytotic spikes.

3. Surface treatments for improving cellular adhesion

Though MDOCs were perfectly adequate from an electrochemical point of view, they required further treatments of their surfaces which were carried out for two reasons. A first factor claiming for proper surface treatment is directly linked to the biological relevance of studies. Indeed, depositing the cells into a device implies a sequence of handling steps (transfection, splitting, change of medium from culture to physiological one, etc.) that stress the cells. In other words, cells need to be cultured onto the microsystem at least for one or two days for retrieving their basic functions so that investigations make sense from a biological point of view. For example, Gillis and co-workers [21] reported the treatment of an ITO device designed for exocytosis detection with poly-L-lysin without alteration of electrochemical responses. A second reason is related to the structure of the microdevice itself. Indeed, microdevices for exocytosis generally involve different surfaces (electrode material, glass or photoresist; see for instance references [17–20,22,25,26,30,31,33]). Even for cells that does not necessarily need a treatment for cell attachment, a homogenization of the whole surface towards cell adhesion is thus preferable, since the membrane affinity could depend on the nature of the surface.

MDOCs were first submitted to an oxygen plasma treatment in order to confer enough hydrophilicity to the SU-8 resist surface and thus creating a viable environment for cells deposited all over the microchip [39]. However, this resulted not sufficient for proper cellular adhesion

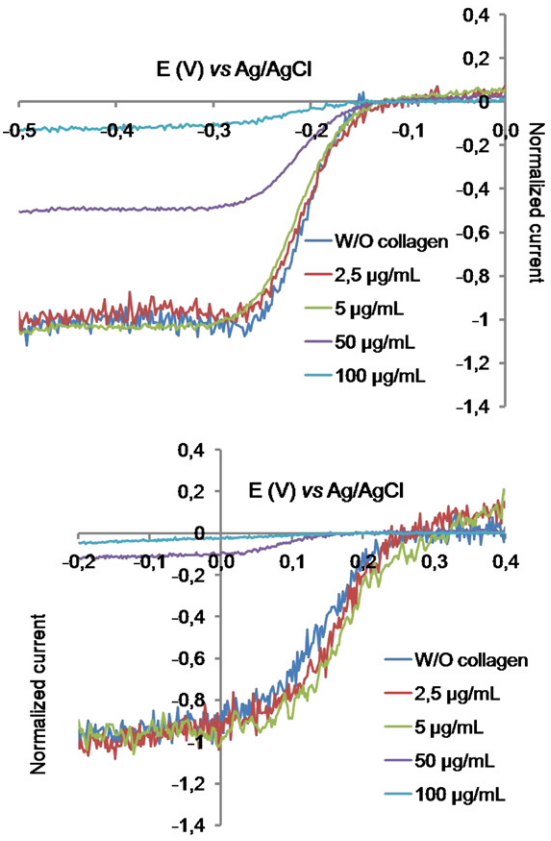

Fig. 4. Representative voltammograms (20 $mV.s^{-1}$) illustrating the effect of collagen coating (evaporation of 250 µL droplets) performed at increasing concentrations (0; 2.5; 5; 50 and 100 $\mu g.mL^{-1}$) on the reduction wave of 1 mM $Ru(NH_3)_6^{3+}$ (top) or $Fe(CN)_6^{3-}$ (bottom) (in physiological buffer of Locke's solution) on ITO band electrodes for MDOC C. Considering the treated surface of our chamber, such concentrations can be converted as 0.13; 0.26; 2.6 and 5.2 $\mu g.cm^{-2}$ coverage densities (see text) respectively.

Table 1
Effects of collagen treatment of ITO surface on the electrochemical current magnitude and slope of the $E = f\left(\log\frac{i_{lim}-i}{i}\right)$ linear correlation for $Ru(NH_3)_6^{3+/2+}$ and $Fe(CN)_6^{3-/4-}$ redox couples and comparison with carbon fiber ultramicroelectrode. nd* = not determined because the signal to noise was too low for a precise analysis. The three concentrations (5 μg.mL^{-1}; 0.05 mg.mL^{-1} and 0.1 mg.mL^{-1}) corresponds to coverage densities values of 0.26; 2.6 and 5.2 μg.cm^{-2} coverage densities respectively (see text).

Electrode	Ru $(NH_3)_6^{3+/2+}$	Fe $(CN)_6^{3-/4-}$	Current intensity plateau as compared with untreated ITO
Carbon	61 mV	96 mV	Not relevant
Naked ITO	58 mV	103 mV	–
ITO coated with 5 μg.mL^{-1} collagen solution	56 mV	100 mV	Identical
ITO coated with 0.05 mg.mL^{-1} collagen solution	56 mV	103 mV	Decrease (two-fold for $Ru(NH_3)_6^{3+/2+}$ and ten-fold for $Fe(CN)_6^{3-/4-}$)
ITO coated with 0.1 mg.mL^{-1} collagen solution	nd*	nd*	Decrease (ten-fold for $Ru(NH_3)_6^{3+/2+}$ and no current for $Fe(CN)_6^{3-/4-}$)

over the exposed ITO surfaces during one- to two-days periods. These were thus further treated with collagen (type IV). Nevertheless, Cui et al., [18] reported through voltammetric investigations that collagen coating altered the electrochemical properties of Au microelectrodes devices. We thus investigated whether or not electrochemical properties of ITO electrodes are affected by collagen treatment. For this we resorted to voltammetric investigations using two well characterized redox systems ($Ru(NH_3)_6^{3+/2+}$ and $Fe(CN)_6^{3-/4-}$).

Voltammetric experiments were performed in solutions of the redox species at 1 mmol.L^{-1} concentration and a scan rate of 20 mV.s^{-1} to allow recording of quasi-steady state voltammograms (Fig. 4) [40]. 250 μL of different collagen concentrations (2.5; 5; 50 and 100 μg.mL^{-1}) solutions was used for coating of ITO microelectrodes, thus resulting as a calculated coverage density of 0.13; 0.26; 2.6 and 5.2 μg.cm^{-2} respectively in our 2.2 × 2.2 cm chamber. This double series of experiments evidenced that the collagen film did not alter electrochemical detection at ITO microelectrodes coated with collagen concentrations up to 5 μg.mL^{-1} (i.e. 0.26 μg.cm^{-2}). However, at larger concentration values and thus higher coverage densities, the intensity of the measured current decreased. This observation is then in full agreement with the report by Cui et al. who used 200 μL at a 200 μg.mL^{-1} collagen concentration to coat their gold microelectrodes array (1.4 × 1.4 cm chamber, thus resulting in a collagen coverage density of 20.4 μg.cm^{-2}), hence observing a decrease of the $Fe(CN)_6^{3-}$ reduction peaks intensity by at least half [18].

Logarithmic analyses of the quasi-stationary voltammograms recorded at 20 mV.s^{-1} for $Ru(NH_3)_6^{3+/2+}$ and $Fe(CN)_6^{3-/4-}$ systems were also performed for further certifying the excellent electrochemical properties of ITO electrodes treated with collagen at concentrations up to 5 μg.mL^{-1} in our experimental conditions. Indeed, for simple electron transfers (as for $Ru(NH_3)_6^{3+/2+}$ and $Fe(CN)_6^{3-/4-}$ redox couples at well-behaved electrodes), logarithmic analysis of electrochemical waves obeys the following relationship:

$$E = E^0 + \frac{0.059}{a} \times \log\frac{i_{lim}-i}{i}$$

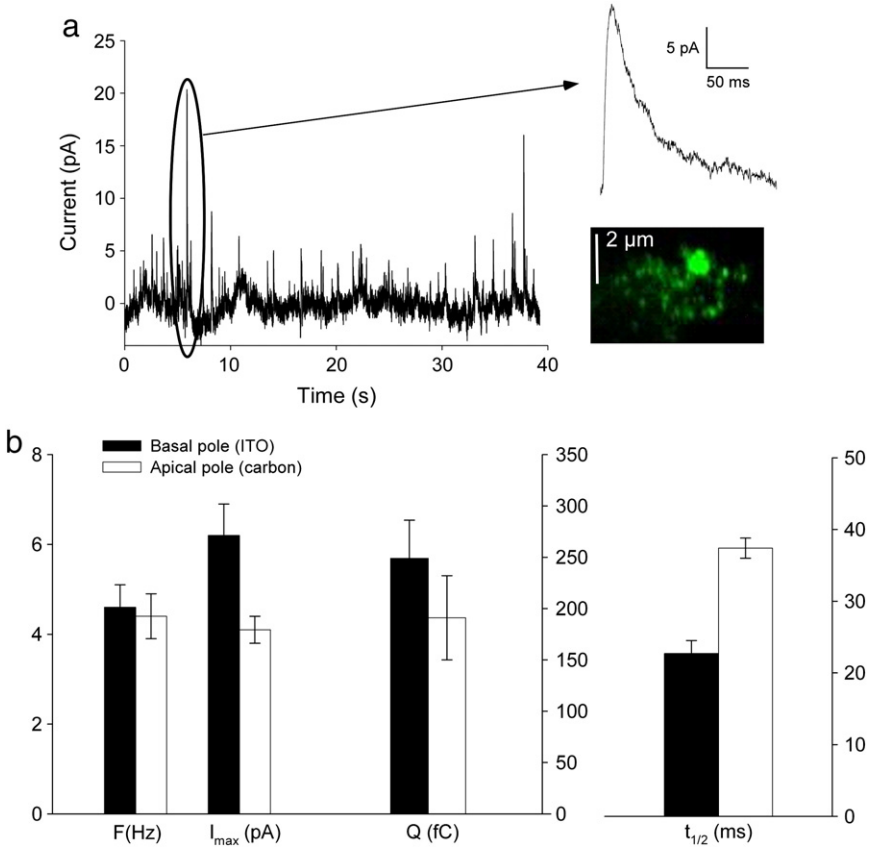

Fig. 5. a) Representative amperometric trace monitored on MDOC C microdevice seeded with BC21 BON cells (see supporting information for details). Insets: a typical amperometric spike (extracted from the trace) and a TIRFM image of an isolated BC21 BON cell (obtained with the MDOC C device) are displayed. For this image, the vesicles are depicted as green points due to the fluorescence of the Green Fluorescent Protein contained into the granules (see details in supplementary information). b) Usual parameters extracted from the amperometric trace (frequency F, charge Q, maximum current I_{max} and half-width time $t_{1/2}$) for electrochemical detection of BC21 cells with MDOC (black; n = 20 cells and 95 corresponding spikes) or carbon fiber (gray; n = 24 cells and 108 corresponding spikes). All values are given as mean ± standard error of the mean (see supporting information).

Table 2
Illustrative list of microsystems devoted to electrochemical detection of exocytosis. The microdevices are classified as a function of their geometry. The cell model investigated, the electrode material and the purpose (combinatory or single analysis cell) are mentioned.

Geometry	Cell analysis	Cell model	Electrode material	References
Array of 25 disk microelectrodes (10 to 90 μm diameter)	Combinatory analysis	MN9D, PC12	Gold	[17,18]
Array of 4 disk microelectrodes (30 μm diameter)	Combinatory analysis	Chromaffin	Nanocrystalline diamond	[19,20]
Array of 24 microelectrodes (20×20 μm square) delimited by opened channels	Combinatory analysis or single cell	Chromaffin	ITO	[22]
Single microelectrode (20×100 μm) located into a microfluidic channel	Combinatory analysis	Chromaffin	ITO	[21]
Array of 8 independant microelectrodes (5×10 μm) into a narrow microfluidic channel	Single cell	PC12	Gold	[23]
Array of 16 microelectrodes (30×40 μm) into a microfluidic channel	Combinatory analysis	Chromaffin	Nitrogen-doped diamond-like carbon	[24]
Circular well (50 to 100 μm)	Single cell	Chromaffin, PC12	Platinum, ITO, Carbon nanotubes deposited on ITO,	[25,26,33]
Array of 16 microfluidic traps (10×15 μm)	Single cell	Chromaffin	Platinum	[46]
Array of 4×10 circular wells (20 μm diameter)	Combinatory analysis or single cell	Chromaffin	Diamond-like carbon	[27,29]
Array of 4 bands (200×700 μm)	Combinatory analysis or single cell	BON	ITO	[32]
Four electrodes array into a well (about 10 μm diameter)	Single cell analysis: mapping	Chromaffin	Single crystallinge diamond, platinum	[20,30,31]

where E (V) is the electrode potential, E^0 (V) the standard potential of the redox couple, i (A) the current measured at potential E, i_{lim} (A) the limiting plateau current of the steady voltammetric wave, and α the transfer coefficient which characterizes the slowness of the redox system ($\alpha = 1$ for a fast redox couple) [41]. The ensuing results for the two systems and different collagen concentrations are summarized in Table 1 and compared to data obtained at usual carbon fiber (10 μm diameter) ultramicroelectrodes. For carbon fiber, untreated or collagen-coated ITO at low collagen concentrations (<5 $\mu g.mL^{-1}$), linear logarithmic analyses were obtained (see Supporting Information) with identical slopes values in the three cases, viz., 58 to 61 mV ($\alpha \approx 1$) and 96 to 103 mV ($\alpha \approx 0.59$) for $Ru(NH_3)_6^{3+/2+}$ and $Fe(CN)_6^{3-/4-}$ systems respectively, in agreement with literature data, i.e., corresponding to a fast redox couple for $Ru(NH_3)_6^{3+/2+}$ and a slow one for $Fe(CN)_6^{3-/4-}$. It has to be emphasized that even for high collagen concentrations, the slope values gave α values that remained close to 1 and 0.59 respectively, thus suggesting that concentrated collagen deposits block irregularly the electrode surface access by forming insulating patches [42].

The observation of a threshold effect of the collagen treatment may be related to collagen structure. Indeed, the collagen structure, composed of three polypeptidic chains associated in a triple helix, notably depends on the coating concentration for given experimental conditions [43]. Then, H. Maeda studied collagen assemblies formed by evaporation (50 μL droplets) at glass substrates for different solutions. In this work, for low concentrations (~0.3 $\mu g.cm^{-2}$),[44] collagen builds a non organized fibrils network (of 50 up to 200 nm thickness) that, by linking with cell membrane proteins, improves cellular adhesion. For intermediate concentrations (3 $\mu g.cm^{-2}$), fibrils start reaching a higher level of organization by lying parallel to each other. At higher concentrations (above 40 $\mu g.cm^{-2}$), fibrils build up lines until reaching a film formation at 120 $\mu g.cm^{-2}$. These investigations are qualitatively consistent with our observations and suggest that under our conditions, collagen fibrils are not associated and remain sufficiently spaced for not hindering diffusion of electroactive molecules towards ITO electrode surfaces irrespective of the species charge. Conversely, at higher collagen concentrations, collagen fibrils cover electrode surfaces, progressively hindering it.

Finally, treatment in our case with a moderate collagen concentration (less than 5 $\mu g.mL^{-1}$, i.e., 0.26 $\mu g.cm^{-2}$) thus resulted perfectly adequate for allowing excellent analytical detection of amperometric traces (see Fig. 5). Indeed, secretion of single BON cells has been amperometrically recorded on MDOC C and usual kinetic or quantitative parameters have then been extracted (see details in Supporting Information). It has to be emphasized that several parameters could differ from those obtained with usual carbon fiber amperometry. This difference between secretion at the top of the cell (with CFA) and the bottom (with the device) has already been observed elsewhere [45].

4. Conclusion

This work reports the microfabrication of several electrode geometries for microsystems devoted to the amperometric detection of cell exocytosis on transparent ITO microelectrodes. Among these geometries, the most satisfactory one involved a spiraling microchannel delimiting squared ITO microelectrodes. This configuration provided electrochemical properties with a suitably low noise while offering an easy seeding of cells by driving them onto the exposed ITO surface. A special attention was given to the effect of collagen surface treatment required for ensuing a proper cell adhesion. We investigated how collagen filming of the ITO active surfaces affected the electrochemical detection. This evidenced that high collagen deposited could drastically decrease the electrochemical response of the device but that moderate collagen coatings were amply sufficient for cell adhesion and exocytosis investigations without altering the electrochemical properties of the device.

As already described above, carbon fiber amperometry currently presents several disadvantages related to the single cell level detection and thus a low-throughput electrochemical recordings. Table 2 summarizes recent contributions reporting the use of microsystems for electrochemical detection of exocytosis. Among them, several works are devoted to overcome such a limitation by allowing a combined electrochemical analysis of several cells or a cell population. As a comparison, our ITO device can be classified as a versatile microdevice since it is able to track exocytosis at the level of the single cell or a cell population, depending on the way to stimulate the cells (see supporting information). Moreover, ITO material has generally been evidenced as suitable for fluorescence detection of exocytosis, [22,32,33], that is also the case of our device (see Fig. 5a), future applications of these microsystems in experiments using fluorescence microscopy could be envisioned.

5. Materials and methods

5.1. Amperometric and voltammetric detections

Amperometric evaluation of the electrical noise at ITO microelectrodes was achieved using a picoamperometer (model AMU-130, Radiometer Analytical Instruments, Copenhagen, DK) at a constant

potential E = + 0.65 V vs. a silver/silver chloride reference electrode (Ag/AgCl). The time course of the amperometric current was monitored (output digitized at 40 kHz) until the baseline reaches a constant value and stored on a computer (Latitude D600, Dell) through a D/A converter (Powerlab 4SP, ADInstruments) and its software interface (Chart version 4.2 for Windows, ADInstruments).

For voltammetry experiments, the concentration of the analytes ($Ru(NH_3)_6^{3+}$ or $Fe(CN)_6^{3-}$) was 10^{-3} mol.L^{-1}. The solutions were freshly prepared in Locke's solution (5.6 mM Glucose, 3.6 mM HCO_3^-, 159.6 mM Cl^-, 157.6 mM Na^+, 5.6 mM K^+, 5 mM Hepes-NaOH, 2.5 mM $CaCl_2$, 1.2 mM $MgCl_2$).

Voltammetric analyses were carried out in a Petri dish using standard three-electrode configuration with a EA162 Picostat (eDAQ, Australia) through a e-corder 401 system associated with EChem sofware. The reference electrode was a silver/silver chloride reference electrode (Ag/AgCl). The auxiliary electrode was a platinum wire.

5.2. ITO microdevice fabrication

For the MDOC A, B and C (see Fig. 2 and Table 1 in Supporting Information), the first steps of the fabrication were identical up to the chemical etching of ITO by HCl (see below).

A thin film of ITO (150 nm thickness; ACM, Villiers Saint Frédéric, France) sputtered onto optical glass slides (22 mm × 22 mm × 0.13 mm) was selected in order to afford a material of low refraction index (1.52) and low electrical resistance (≤20 ohms per square). The microelectrode band-array of ITO was manufactured using photolithography processes. The ITO slide was cleaned with acetone and deionised water, then dried with filtered compressed air, afterwards treated with oxygen plasma at 350 mTorr (100 W) (Harrick Plasma, NY, USA) for 1 min to remove all dust on it. The protocol for fabrication of the microchip is the following. First, an insulating layer of photoresist AZ 9260 (Clariant GmbH, Wiesbaden, Germany) was patterned onto the ITO/glass slides: spin-coating (3800 rpm, 500 rpm.s^{-1}, 30 s), pre-bake on a hotplate (2 min at 110 °C) to vaporize solvent, exposure to UV light through a specific mask design (900 mJ.cm^{-2}), development in a bath of AZ 400 K/H_2O (2/1) (Clariant GmbH, Wiesbaden, Germany) for 30 s, rinsed with deionised water and dried with filtered compressed air. Then, the ITO with no "photoresist protective layer" was chemically etched by using commercial HCl solution (37% volume, Sigma-Aldrich, Saint-Quentin Fallavier, France) (6–7 min) and the photoresist was directly removed with acetone. Later the slide is rinsed, dried and treated again by oxygen plasma in the same conditions than above. Now, in order to control the active zone of microelectrode array, a 10 μm thick film is obtained by spin-coating 1 ml of SU-8 3010 (MicroChem®) at 3000 rpm with a 300 rpm.s^{-1} acceleration for 30 s. The resist was then soft baked for 2 min at 65 °C and 3 min at 95 °C. Then, it was exposed to UV light through another specific mask design (100 mJ.cm^{-2}) and post-baked for 1 min at 65 °C and 3 min at 95 °C. Finally, the resist was developed in a bath of propylene glycol methyl ether acetate (PGMEA) for 1 min and rinsed in isopropanol (IPA) and water.

Then the only differences for MDOC A, B, and C concerned the design of the optical masks used in order to control the active zone of microelectrode array (see Fig. 2).

The microchip is finally fixed on a Petri dish, by using a silicone rubber (3140 RTV coating, Dow Corning®), compatible with the TIRF microscope set-up and previously holed.

For subsequent cell experiments, devices are covered with 250 μL of different concentrations of Type IV collagen (2.5; 5; 50 and 100 μg.mL^{-1}) solutions supplemented with 30% ethanol. After 3 h of evaporation, dishes were washed with 1 mL of PBS, and stored at 4 °C.

Acknowledgments

This work has been supported in part by CNRS (UMR 8640, FR2702, LIAXiamENS), Ecole Normale Supérieure, French Ministry of Research, Université Pierre & Marie Curie Paris 06, and by the European Commission under the Seventh Framework Programme (Nanoscale CP-FP 214566-2).

Appendix A. Supplementary data

Supplementary data to this article can be found online at doi:10.1016/j.bpc.2011.12.002.

References

[1] R.D. Burgoyne, A. Morgan, Secretory granule exocytosis, Physiological Reviews 83 (2003) 581–632.
[2] S.C. Ge, S. Koseoglu, C.L. Haynes, Bioanalytical tools for single-cell study of exocytosis, Analytical and Bioanalytical Chemistry 397 (2011) 3281–3304.
[3] D.M. Omiatek, A.S. Cans, M.L. Heien, A.G. Ewing, Analytical approaches to investigate transmitter content and release from single secretory vesicles, Analytical and Bioanalytical Chemistry 397 (2010) 3269–3279.
[4] L. Mellander, A.S. Cans, A.G. Ewing, Electrochemical probes for detection and analysis of exocytosis and vesicles, Chemphyschem 11 (2010) 2756–2763.
[5] C. Amatore, S. Arbault, M. Guille, F. Lemaître, Electrochemical monitoring of single cell secretion: vesicular exocytosis and oxidative stress, Chemical Reviews 108 (2008) 2585–2621.
[6] A.G. Teschemacher, Real-time measurements of noradrenaline release in periphery and central nervous system, Autonomic Neuroscience-Basic & Clinical 117 (2005) 1–8.
[7] C. Fernandez-Peruchena, S. Navas, M.A. Montes, G.A. de Toledo, Fusion pore regulation of transmitter release, Brain Research Reviews 49 (2005) 406–415.
[8] R. Borges, M. Camacho, K.D. Gillis, Measuring secretion in chromaffin cells using electrophysiological and electrochemical methods, Acta Physiologica 192 (2008) 173–184.
[9] E.R. Travis, R.M. Wightman, Spatio-temporal resolution of exocytosis from individual cells, Annual Review of Biophysics and Biomolecular Structure 27 (1998) 77–103.
[10] R.M. Wightman, Probing cellular chemistry in biological systems with microelectrodes, Science 311 (2006) 1570–1574.
[11] C.A. Aspinwall, S.A. Brooks, R.T. Kennedy, J.R.T. Lakey, Effects of intravesicular H+ and extracellular H+ and Zn2+ on insulin secretion in pancreatic beta cells, Journal of Biological Chemistry 272 (1997) 31308–31314.
[12] R.T. Kennedy, L. Huang, M.A. Atkinson, P. Dush, Amperometric monitoring of chemical secretions from individual pancreatic beta-cells, Analytical Chemistry 65 (1993) 1882–1887.
[13] W. Wang, S.H. Zhang, L.M. Li, Z.L. Wang, J.K. Cheng, W.H. Huang, Monitoring of vesicular exocytosis from single cells using micrometer and nanometer-sized electrochemical sensors, Analytical and Bioanalytical Chemistry 394 (2009) 17–32.
[14] C. Spegel, A. Heiskanen, L.H.D. Skjolding, J. Emneus, Chip based electroanalytical systems for cell analysis, Electroanalysis 20 (2008) 680–702.
[15] G. Velve-Casquillas, M. Le Berre, M. Piel, P.T. Tran, Microfluidic tools for cell biological research, Nano Today 5 (2010) 28–47.
[16] Y. Huang, D. Cai, P. Chen, Micro- and nanotechnologies for study of cell secretion, Analytical Chemistry 83 (2011) 4393–4406.
[17] H.F. Cui, J.S. Ye, Y. Chen, S.C. Chong, X. Liu, T.M. Lim, F.S. Sheu, In situ temporal detection of dopamine exocytosis from L-dopa-incubated MN9D cells using microelectrode array-integrated biochip, Sensors and Actuators B-Chemical 115 (2006) 634–641.
[18] H.F. Cui, J.S. Ye, Y. Chen, S.C. Chong, F.S. Sheu, Microelectrode array biochip: Tool for in vitro drug screening based on the detection of a drug effect on dopamine release from PC12 cells, Analytical Chemistry 78 (2006) 6347–6355.
[19] V. Carabelli, S. Gosso, A. Marcantoni, Y. Xu, E. Colombo, Z. Gao, E. Vittone, E. Kohn, A. Pasquarelli, E. Carbone, Nanocrystalline diamond microelectrode arrays fabricated on sapphire technology for high-time resolution of quantal catecholamine secretion from chromaffin cells, Biosensors & Bioelectronics 26 (2010) 92–98.
[20] A. Pasquarelli, V. Carabelli, Y.L. Xu, E. Colombo, Z.Y. Gao, J. Scharpf, E. Carbone, E. Kohn, Diamond microelectrodes arrays for the detection of secretory cell activity, International Journal of Environmental and Analytical Chemistry 91 (2011) 150–160.
[21] X.H. Sun, K.D. Gillis, On-chip amperometric measurement of quantal catecholamine release using transparent indium tin oxide electrodes, Analytical Chemistry 78 (2006) 2521–2525.
[22] X.H. Chen, Y.F. Gao, M. Hossain, S. Gangopadhyay, K.D. Gillis, Controlled on-chip stimulation of quantal catecholamine release from chromaffin cells using photolysis of caged Ca2+ on transparent indium-tin-oxide microchip electrodes, Lab on a Chip 8 (2008) 161–169.
[23] G.M. Dittami, R.D. Rabbitt, Electrically evoking and electrochemically resolving quantal release on a microchip, Lab on a Chip 10 (2010) 30–35.
[24] Y.F. Gao, X.H. Chen, S. Gupta, K.D. Gillis, S. Gangopadhyay, Magnetron sputtered diamond-like carbon microelectrodes for on-chip measurement of quantal catecholamine release from cells, Biomedical Microdevices 10 (2008) 623–629.
[25] B.X. Shi, Y. Wang, T.L. Lam, W.H. Huang, K. Zhang, Y.C. Leung, H.L.W. Chan, Release monitoring of single cells on a microfluidic device coupled with fluorescence microscopy and electrochemistry, Biomicrofluidics 4 (2010) 043009.

[26] B.X. Shi, Y. Wang, K. Zhang, T.L. Lam, H.L.W. Chan, Monitoring of dopamine release in single cell using ultrasensitive ITO microsensors modified with carbon nanotubes, Biosensors & Bioelectronics 26 (2011) 2917–2921.
[27] S. Barizuddin, X. Liu, J.C. Mathai, M. Hossain, K.D. Gillis, S. Gangopadhyay, Automated targeting of cells to electrochemical electrodes using a surface chemistry approach for the measurement of quantal exocytosis, ACS Chemical Neuroscience 1 (2010) 590–597.
[28] P. Chen, B. Xu, N. Tokranova, X.J. Feng, J. Castracane, K.D. Gillis, Amperometric detection of quantal catecholamine secretion from individual cells on micromachined silicon chips, Analytical Chemistry 75 (2003) 518–524.
[29] X. Liu, S. Barizuddin, W. Shin, C.J. Mathai, S. Gangopadhyay, K.D. Gillis, Microwell device for targeting single cells to electrochemical microelectrodes for high-throughput amperometric detection of quantal exocytosis, Analytical Chemistry 83 (2011) 2445–2451.
[30] A.F. Dias, G. Dernick, V. Valero, M.G. Yong, C.D. James, H.G. Craighead, M. Lindau, An electrochemical detector array to study cell biology on the nanoscale, Nanotechnology 13 (2002) 285–289.
[31] I. Hafez, K. Kisler, K. Berberian, G. Dernick, V. Valero, M.G. Yong, H.G. Craighead, M. Lindau, Electrochemical imaging of fusion pore openings by electrochemical detector arrays, Proceedings of the National Academy of Sciences of the United States of America 102 (2005) 13879–13884.
[32] A. Meunier, O. Jouannot, R. Fulcrand, I. Fanget, M. Bretou, E. Karatekin, S. Arbault, M. Guille, F. Darchen, F. Lemaître, C. Amatore, Coupling amperometry and total internal reflection fluorescence microscopy at ITO surfaces for monitoring exocytosis of single vesicles, Angewandte Chemie International Edition 50 (2011) 5081–5084.
[33] C. Amatore, S. Arbault, Y. Chen, C. Crozatier, F. Lemaître, Y. Verchier, Coupling of electrochemistry and fluorescence microscopy at indium tin oxide microelectrodes for the analysis of single exocytotic events, Angewandte Chemie International Edition 45 (2006) 4000–4003.
[34] A. Sen, S. Barizuddin, M. Hossain, L. Polo-Parada, K.D. Gillis, S. Gangopadhyay, Preferential cell attachment to nitrogen-doped diamond-like carbon (DLC:N) for the measurement of quantal exocytosis, Biomaterials 30 (2009) 1604–1612 and references therein.
[35] C. Guillen, J. Herrero, Comparison study of ITO thin films deposited by sputtering at room temperature onto polymer and glass substrates, Thin Solid Films 480 (2005) 129–132.
[36] W.Y. Guo, J.J. Li, H.H. Chu, J.L. Yan, Y.F. Tu, Studies on the electrochemiluminescent behavior of luminol on indium tin oxide (ITO) glass, Journal of Luminescence 130 (2010) 2022–2025.
[37] Y. Kim, J. Do, E. Kim, G. Clavier, L. Galmiche, P. Audebert, Tetrazine-based electrofluorochromic windows: modulation of the fluorescence through applied potential, Journal of Electroanalytical Chemistry 632 (2009) 201–205.
[38] H. Li, Y.J. Liu, J.A. Xu, Z.H. Xu, L.N. Ji, W.S. Li, H.Y. Chen, DNA-enhanced assembly of [Ru(bpy)(2)ITATP](3+/2+) on an ITO electrode, Electrochimica Acta 52 (2007) 4956–4961.
[39] M. Hennemeyer, F. Walther, S. Kerstan, K. Schurzinger, A.M. Gigler, R.W. Stark, Cell proliferation assays on plasma activated SU-8, Microelectronic Engineering 85 (2008) 1298–1301.
[40] C. Amatore, Electrochemistry at Ultramicroelectrodes, in: I. Rubinstein (Ed.), Physical Electrochemistry: Principles, Methods and Applications, M. Dekker, New York, 1995, pp. 131–208.
[41] A.J. Bard, L.R. Faulkner, Electrochemical Methods: Fundamentals and Applications, John Wiley and Sons, New York, 2001.
[42] C. Amatore, J.M. Saveant, D. Tessier, Charge-transfer at partially blocked surfaces – a model for the case of microscopic active and inactive sites, Journal of Electroanalytical Chemistry 147 (1983) 39–51.
[43] H. Maeda, An atomic force microscopy study of ordered molecular assemblies and concentric ring patterns from evaporating droplets of collagen solutions, Langmuir 15 (1999) 8505–8513.
[44] In this excellent paper (reference [43]), Maeda's investigations were achieved by considering different collagen concentrations in solution ($\mu g.mL^{-1}$) and not coverage densities ($\mu g.cm^{-2}$). Unfortunately, the glass area covered by the collagen solution during the evaporation was not mentioned. In order to globally compare with our results, we roughly estimate (by depositing 50 μL droplets of relevant collagen concentrations on glass slides) such a surface as a 1 cm diameter disc. It thus allows obtaining approximated coverage densities for a qualitative comparison.
[45] C. Amatore, S. Arbault, F. Lemaître, Y. Verchier, Comparison of apex and bottom secretion efficiency at chromaffin cells as measured by amperometry, Biophysical Chemistry 127 (2007) 165–171.
[46] Y.F. Gao, S. Bhattacharya, X.H. Chen, S. Barizuddin, S. Gangopadhyay, K.D. Gillis, A microfluidic cell trap device for automated measurement of quantal catecholamine release from cells, Lab on a Chip 9 (2009) 3442–3446.